Cell Reports, Volume *24*

Supplemental Information

Loss of Nucleobindin-2 Causes Insulin Resistance in Obesity without Impacting Satiety or Adiposity

Anthony Ravussin, Yun-Hee Youm, Jil Sander, Seungjin Ryu, Kim Nguyen, Luis Varela, Gerald I. Shulman, Sviatoslav Sidorov, Tamas L. Horvath, Joachim L. Schultze, and Vishwa Deep Dixit

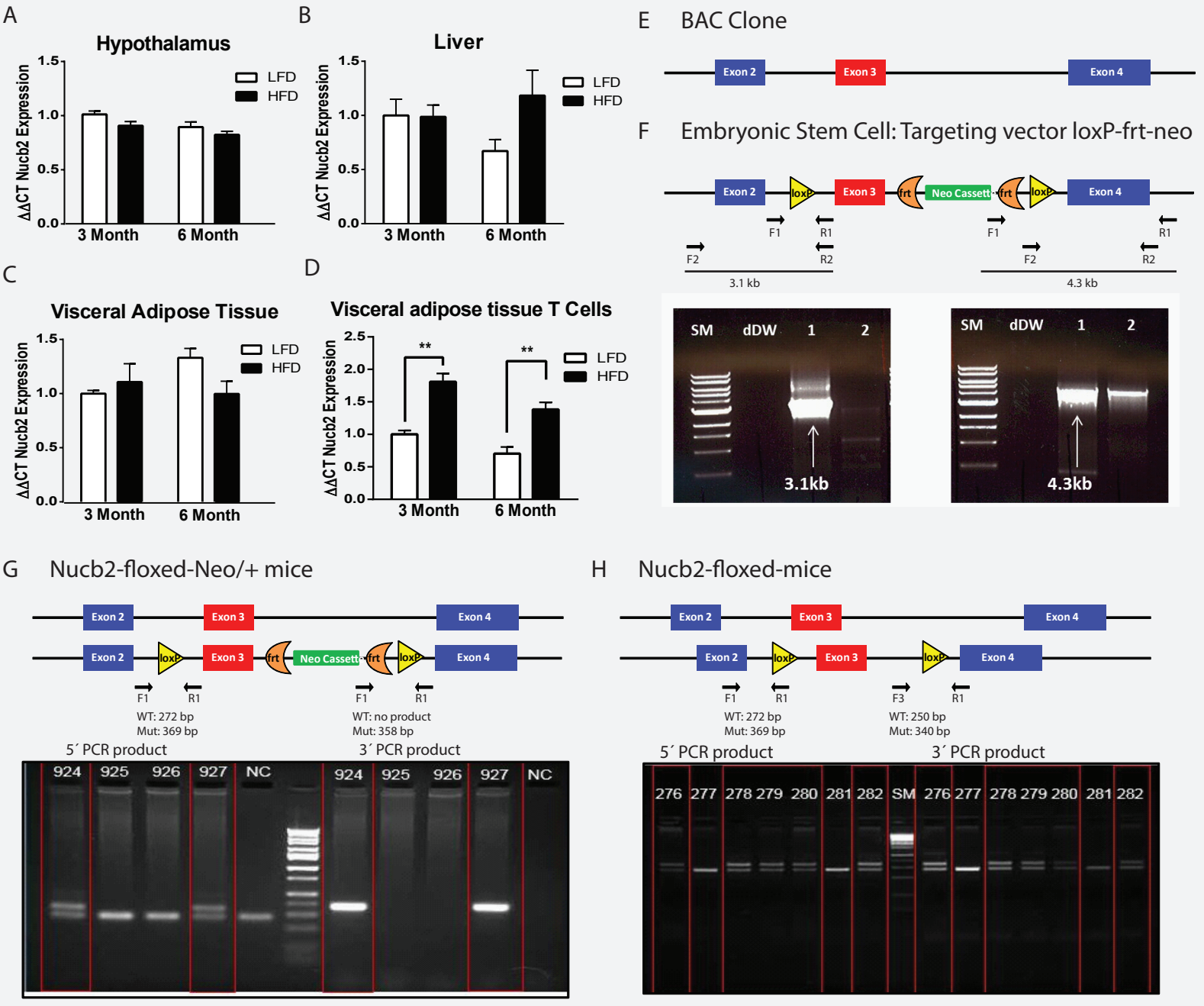

Supplemental Figure 1. Nucb2 expression in response to high-fat diet and method of generation, characterization of Nucb2 floxed mice (Related to Figure 1A).

Realtime PCR analysis of *Nucb2* mRNA in **(A)** Hypothalamus, **(B)** Liver **(C)** Visceral Adipose Tissue and **(D)** CD3+ adipose tissue T cells in mice fed normal chow or a 60% HFD (n=6/group). **(E)** *Nucb2* KO construct design **(F)** Embryonic Stem Cell Targeting Vector and PCR validation. **(G)** PCR validation of floxed-Neo/+ mice. **(H)** PCR validation of floxed heterozygous mice.

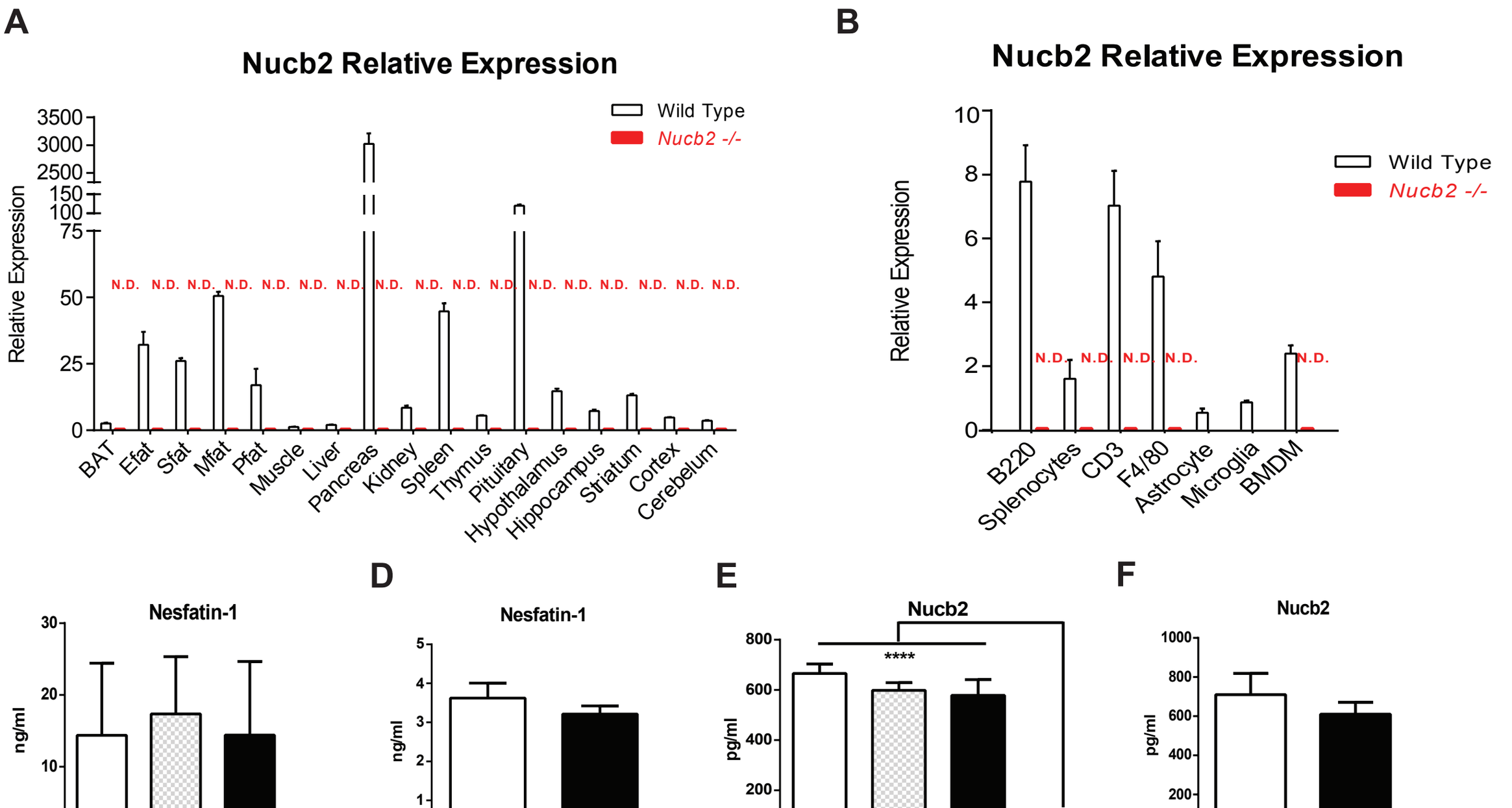

Supplemental Figure 2. Characterization of Nucb2 and Nesfatin-1 expression in tissues and sera and metabolic parameters in Nucb2 deficient mice (Related to Figure 1B).

Realtime PCR analysis of *Nucb2* mRNA in **(A)** Tissular and **(B)** cellular expression of *Nucb2* mRNA in WT and *Nucb2*$^{-/-}$ mice (n=4/group). Plasma nesfatin-1 and *Nucb2* (CUSA Bio) post-translational peptide ELISAs non-specifically detects the peptide in chow fed, 12 week old mice lacking *Nucb2* in fed or fasted state **(C and E)** (n=6/group). Spiked samples are the assay diluent (with no biological sample) spiked with (100nM) of recombinant nesfatin-1, nesfatin-2 and nesfatin-3. WT and Nucb2-/- *Nucb2*$^{-/-}$ 10 month old, male mice on a high fat diet **(D and F)** (n=5/group). **(G)** Body weight from 10 month old HFD mice (WT n=8, KO n=5) **(H)** Elimination of *Nucb2* does not regulate food intake in mice fed chow or 60% HFD. Food intake was measured by mass over 72 hours every 12 hours and represented over a 24 hour average (chow, n=8/group HFD, n=5-8/group). **(I)** Lack of *Nucb2* does not regulate AgRP mRNA expression in hypothalamus of fed and fasted mice. **(J, K)** Adipocyte size distribution histogram. The average size of adipocyte was measured by using Image J and averaging over 180 different cells from 4 different mice/strain. **(L)** Body fat. **(M)** Weight of fat pads. Plasma levels of **(N)** Leptin and **(O)** Adiponectin in WT and KO mice.

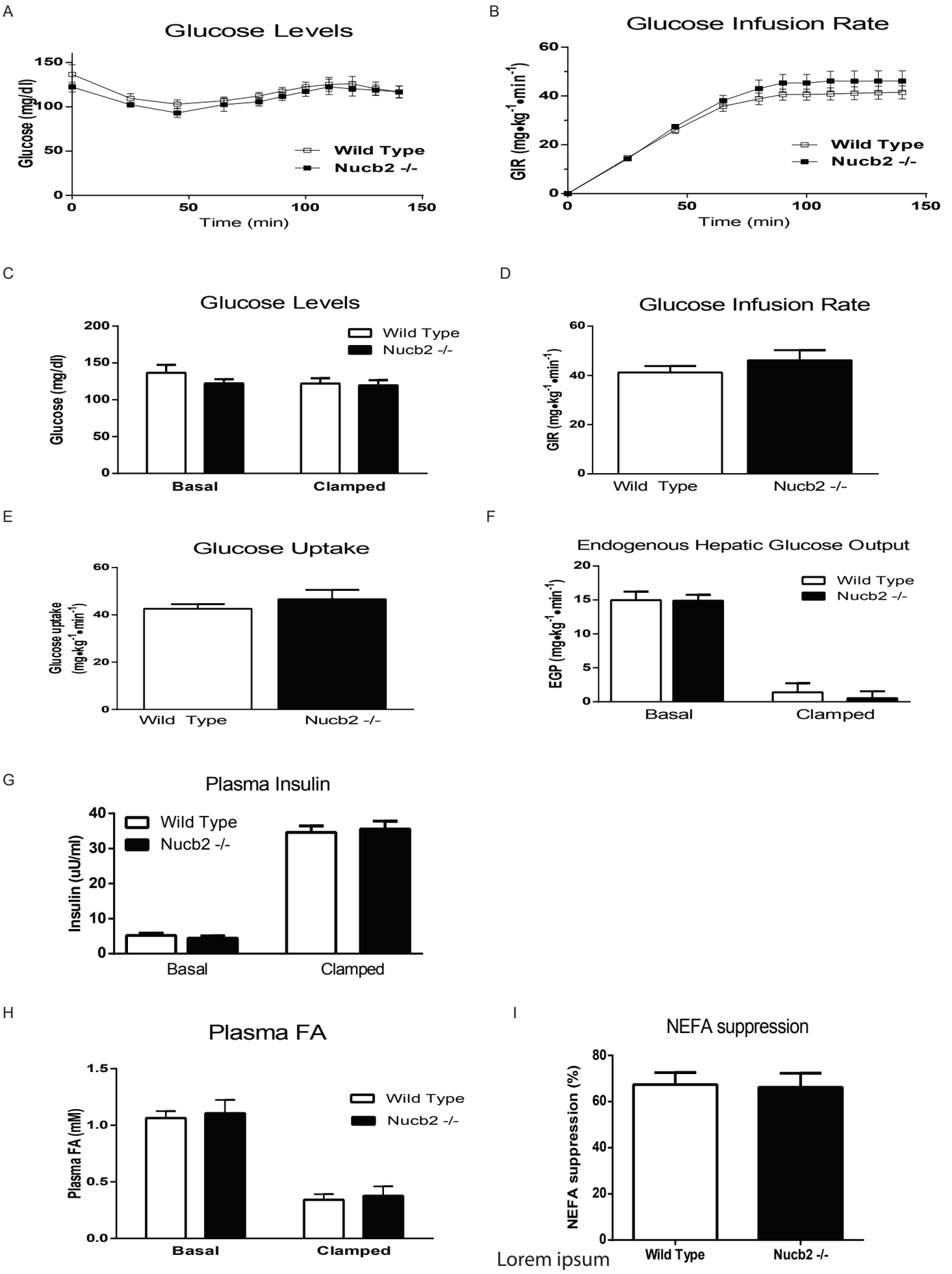

Supplemental Figure 3. Effect of Nucb2 deletion on insulin-sensitivity in mice fed normal chow diet (Related to Figure 2A-F).

(A) Time-course of plasma glucose levels **(B)** Glucose Infusion Rate **(C)** Basal and Clamped plasma glucose levels **(D)** End-point glucose infusion rate **(E)** Systemic glucose uptake during the steady-state period (final 40 min) of the clamp **(F)** and Basal and insulin-stimulated clamped hepatic endogenous glucose production. Male 14 week old chow fed mice and data are represented as mean ± SEM (wild type, n=8 and *Nucb2*$^{-/-}$, n=7) **(G)** Basal and clamped plasma insulin levels **(H)** Basal and insulin-stimulated clamped plasma free fatty acid levels **(I)** NEFA (Non-esterified Fatty Acids) Plasma fatty acid suppression. Data are represented as mean ± SEM (wild type, n=8 and *Nucb2*$^{-/-}$, n=7).

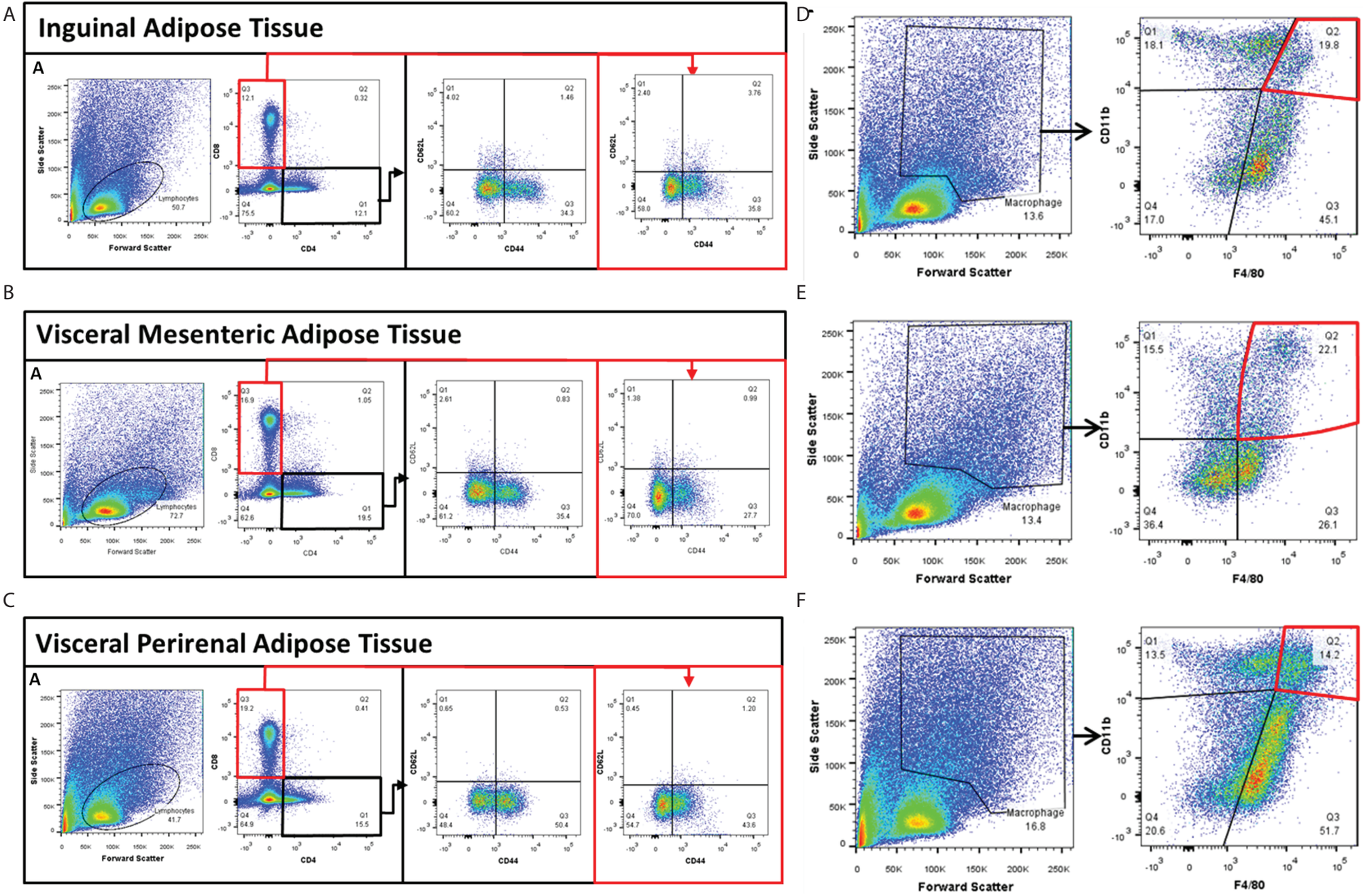

Supplemental Figure 4. Representative FACS plot depicting analysis of adipose tissue macrophages (Related to Figure 2G-J).

Representative flow cytometry dot plots of SVF from subcutaneous inguinal adipose tissue, visceral mesenteric adipose tissue and visceral perirenal adipose. Macrophage populations in **(A)** inguinal adipose tissue, **(B)** visceral mesenteric adipose tissue and **(C)** visceral perirenal adipose tissue gating strategy and macrophage quantifications. Flow gating strategy for lymphoid populations and T cell subset analysis in **(D)** inguinal adipose tissue, **(E)** visceral mesenteric adipose tissue, and **(F)** visceral mesenteric adipose tissue. All data are represented as mean ± SEM (mice are 8 month old, male high fat diet fed wild type, n=5 and *Nucb2*$^{-/-}$, n=8).